Mon. Not. R. astr. Soc. (1981) **195**, *Short Communication*, 29P–32P

X-ray line emission from photo-ionized gas in a Seyfert nucleus

A. C. Fabian *Institute of Astronomy, Madingley Road, Cambridge CB3 0HA*
R. R. Ross *Institute for Advanced Study, Princeton, New Jersey 08540, USA*

Received 1980 December 8

Summary. We show that the strong iron line observed in the *Ariel V* X-ray spectrum of the Seyfert galaxy NGC 5548 may be due to recombination-line emission in a highly photo-ionized gas. This gas must lie within 3×10^{16} cm of the source of the continuum emission, and provides a direct handle on conditions deep within the broad-line region of the nucleus. The iron line is the closest feature yet observed to the continuum source.

1 Introduction

A strong iron emission feature has been found in an *Ariel V* X-ray spectrum of the Seyfert 1 galaxy NGC 5548, taken when the source was at a comparatively low intensity level (Hayes *et al.* 1980). *HEAO-1* observations made 18 months later when the source was about 50 per cent stronger (Mushotzky *et al.* 1980) do not reveal such a feature. Hayes *et al.* (1980) estimate that the line flux on that date was at least three times weaker than that found in their spectrum. They interpret the emission feature as fluorescence from cool gas clouds (with $T \sim 10^4$ K) surrounding the nucleus of NGC 5548, although they cannot exclude other possible sites such as a hot, low-density intracloud medium. The fluorescence interpretation requires a covering factor by clouds that is near unity and a fortunate pattern of variations in the source intensity.

We show here that a strong iron emission feature can occur as a result of recombinations in highly photo-ionized gas surrounding the central source. Iron is the last abundant element to be completely stripped of electrons. For convenience we assume that this gas is in the form of a uniform shell, which could indeed be related to the intracloud medium inferred to occur in galactic nuclei (see e.g. McCray 1979; Blumenthal & Mathews 1979; Ulrich *et al.* 1980; Bergeron 1980; Maraschi, Perola & Treves 1980). The strength of the iron emission does demand, however, that it arises from the innermost parts, $R < 3 \times 10^{16}$ cm, which need not necessarily contain cool clouds. Photo-ionization has the required effect that the line flux increases, at least over a certain range, with decreasing source luminosity.

2 The photo-ionized region

The *Ariel V* X-ray spectrum of NGC 5548 is similar in shape to several theoretical spectra generated by one of us from model Alfvén shells surrounding a neutron star X-ray source

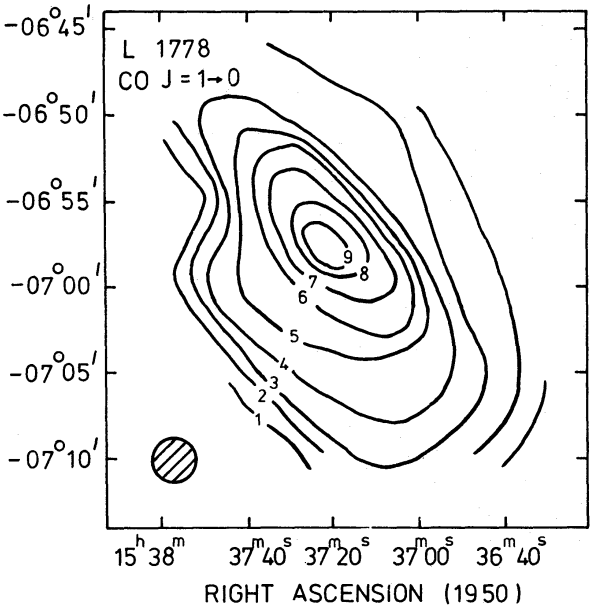

Figure 9. Peak T_A^*(CO) for L1778.

Determining optical depth from

$$\tau(^{13}\mathrm{CO}) \simeq -\ln\left\{1 - \frac{T_A^*(^{13}\mathrm{CO})}{T_A^*(\mathrm{CO})}\right\}, \tag{20}$$

at the (Lynds) location of L1778 we obtain $\tau(^{13}\mathrm{CO}) \sim 0.4$, giving for line width $\Delta V \sim 0.5$ km s^{-1}, excitation temperature $T \simeq 10$ K a column density $N(\mathrm{H_2}) \sim 10^{21}$ cm^{-2} and extinction $A_V \sim 1$ mag, in tolerable agreement with observed extinction levels. For column depth comparable with observed cloud width (~ 20 arcmin) mean density becomes $n(\mathrm{H_2}) \sim 3 \times 10^2$ cm^{-3}. This is well into the density regime where photon-trapping becomes important, and an alternative radiative-transfer procedure based on the analysis of Scoville & Solomon (1974) increases mean values $N(\mathrm{H_2})$, A_V, $n(\mathrm{H_2})$ by a factor ~ 4. Therefore, whilst the central core of L1778 may be characterized by larger values of $n(\mathrm{H_2})$, densities in the enveloping regions are probably quite low. The reduction of temperature in the outer regions of L1778 is unlikely therefore to represent a variation in gas kinetic temperature (see Appendix) so much as a reduced level of CO collisional excitation.

Applying a virial analysis similar to that in the discussion of TMC-1 gives terms $K_{TH} \sim 6.2 \times 10^8$ erg cm^{-3}, $K_{TB} \sim 1.3 \times 10^9$ erg cm^{-3}, $K_R \sim 4.5 \times 10^7$ erg cm^{-3}, $\Omega_G \sim 1.8 \times 10^9$ erg

Table 2. $T_A^*(^{13}\mathrm{CO})$ for L1778.

Position	$T_A^*(^{13}\mathrm{C}^{16}\mathrm{O})$ (K $\pm 2\sigma$)	V (km s^{-1})	ΔV (km s^{-1})
7.5E 0N	<1.3 (0.9)	–	–
0W 2.5N	1.5 (0.5)	3.8	0.6
0W 2.5S	<1.3 (0.5)	–	–
0W 0N	1.7 (0.4)	3.8	0.5
2.5W 2.5N	2.3 (0.8)	3.8	0.6
2.5W 2.5S	2.1 (0.9)	3.9	0.9
5W 5N	1.9 (0.8)	3.8	0.5
5W 2.5N	1.6 (0.8)	3.8	0.5

(Ross 1978, 1979). Whilst no Alfvén shell of the necessarily large size will occur in a galactic nucleus, a shell of gas may represent the densest regions of a surrounding inflow or outflow. In the absence of any detailed model for the gas properties, we have for convenience again assumed a uniform shell of inner radius R, thickness ΔR and density n. The X-rays incident on the inside face of the shell are taken to have an energy spectrum that is constant below 1 keV, a power law of index α between 1 and 100 keV, and zero above that.

The absence of any strong absorption at energies below the iron line implies that C, N, O, S and Si, at least, must be highly ionized. The ionization parameter due to an X-ray ionizing luminosity L_x

$$\xi = (L_x/nR^2)/a_\tau$$

where $a_\tau = \max(1, \tau)$ (Ross 1979) must thus be $\sim 10^3$. L_x is essentially the 1–10 keV luminosity. The iron line luminosity of $\sim 10^{51}$ photon s^{-1}, if due to recombinations at a rate coefficient α_{Fe} ($\sim 10^{-11}\,cm^3\,s^{-1}$), requires

$$n^2R^2\alpha_{Fe}\,4\pi\Delta R\,A_{Fe} \simeq 10^{51},$$

where A_{Fe} is the iron abundance (taken here to be 2.5×10^{-5}). These combine to give an electron scattering optical depth, $\tau = n\Delta R\sigma_T$, of $\simeq 2$ and the product $nR^2 \simeq 10^{41}$, for $L_x = 5 \times 10^{43}\,erg\,s^{-1}$. This is satisfactory from the point of view of linewidth. Values of $\tau > 3$ spread the line profile over many keV, thereby reducing its detectability. The maximum radius of such a region occurs when it is completely filled with gas and is then $\sim 3 \times 10^{16}$ cm.

Fig. 1 shows the results of computations of the self-consistent radiative transfer and ionization structure for a shell of $\tau = 2$, $n = 10^{10}\,cm^{-3}$ and $R = 4 \times 10^{15}$ cm, using the approach outlined in Ross (1978, 1979). We have used here three separate 1–100 keV luminosities

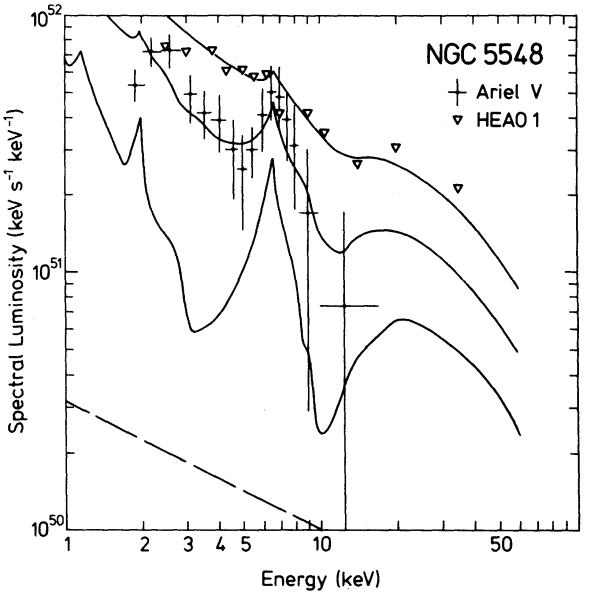

Figure 1. *Ariel V* and *HEAO-1* observations of NGC 5548 compared with model spectra computed on the basis of radiative transfer through a self-consistently photo-ionized shell. The electron density in the shell is $10^{10}\,cm^{-3}$, its inner radius is 4×10^{15} cm and it has an electron-scattering optical depth of 2. The X-ray spectrum incident on the inner face of the shell is a power law of index 0.5 (the same as the dashed line) between 1 and 100 keV. The emergent spectra from three separate luminosities are shown. Narrow unscattered iron-line cores of negligible total intensity are not shown. The heavy elements C, O, Si and Fe are included; the abundance of Si is doubled so that it represents Si and Mg combined. Omission of sulphur in the computations means that the predicted flux is slightly underestimated between ~ 2 and 3 keV.

cm^{-3}, $\Omega_H \sim 3.0 \times 10^8 erg\,cm^{-3}$, where the cloud is assumed homogeneous, of radius $R \sim 1.8 \times 10^{18}$ cm, density $n(H_2) \sim 2 \times 10^3 cm^{-3}$ and has rotational velocity $\omega R \lesssim 0.15\,km\,s^{-1}$. Turbulent velocity is taken to be comparable with observed linewidth ($\sim 0.5\,km\,s^{-1}$) and the magnetic field strength $H \sim 10^{-5}$ G. For these assumptions the cloud is stable against collapse. However, if the turbulent velocity is small and H not significantly larger than the adopted value, gravitational self energy exceeds other contributions, and line width may then be attributable to global contraction (free-fall velocity would be $\sim (2G\mathcal{M}/R)^{1/2} \sim 1\,km\,s^{-1}$). Stability of the cloud is therefore ambiguous, and depends critically upon the interpretation of line broadening.

8 L129

L129 is a Lynds opacity class 6 cloud. The extinction map (Fig. 10) shows it to be an elongated formation of size ~ 10 arcmin, located within a region of slowly varying extinction with $A_V \sim 1$ mag. The CO map (Fig. 11) reveals a broad temperature plateau corresponding to an excitation temperature $T \sim 13$ K, sharply bounded to the south-east and north-west. ^{13}CO observations (Fig. 11) in contrast locate a very much narrower region of temperature enhancement, peaking close to the CO core, and with a characteristic halfwidth ~ 10 arcmin, although there is also evidence for extension along the line of the CO plateau. The ^{13}CO observations, interpreted as a change in column density, therefore identify a core of comparable size and (within uncertainties) location to the high extinction region L129. Using equations (4), (20) for optical depth and column density then gives $\tau(^{13}CO) \sim 0.9$ and $N(^{13}CO) \sim 3.1 \times 10^{15} cm^{-2}$ for $\Delta V \sim 0.5\,km\,s^{-1}$, implying $N(H_2) \sim 2.5 \times 10^{21}$ and characteristic extinction $A_V \sim 2.5$ mag. A radiative-transfer procedure (Section 7) roughly doubles $N(^{13}CO)$, A_V. For either case size is comparable to the Jeans length, and mass $\mathcal{M} \sim 50 \rightarrow 100 \mathcal{M}_\odot$.

L129 appears therefore to contain a possibly pre-stellar core, at a low temperature characteristic of the much larger enveloping cloud. This in turn appears to be essentially

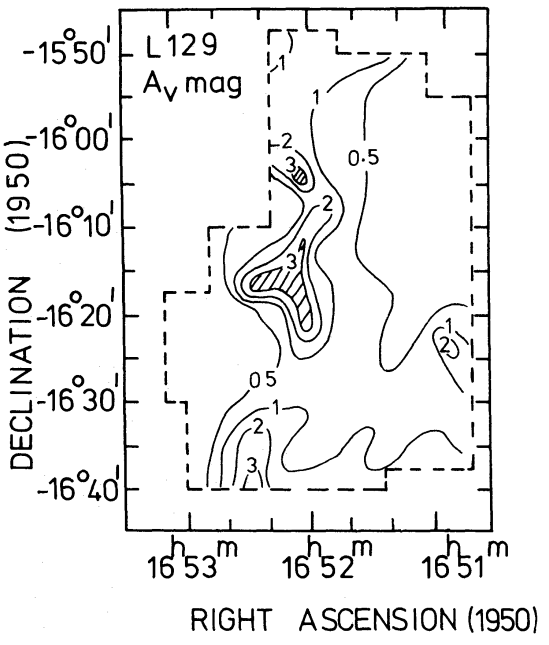

Figure 10. Extinction for region of L129 CO map (Fig. 11).

for an energy power-law index of 0.5. A luminosity of 2×10^{44} erg s^{-1} (1–100 keV) is a reasonable fit to the *Ariel V* data, whilst 3.8×10^{44} erg s^{-1} models the *HEAO-1* result. The observed iron feature is identified as the recombination lines of Fe XXV at 6.7 keV; the large width being due to Comptonization. A small unscattered core is now shown. Reducing the luminosity to 10^{44} erg s^{-1} causes significant recombination of the shell and the appearance of large Comptonized absorption edges. This last spectrum suggests that some active nuclei might be detected only by their line emission.

Several other models have been computed. We find that changes in spectral index can also give reasonable agreement. Shells with $\tau > 3$ result in a line spread much greater than can be consistent with the observations. The results scale as expected between $n = 10^{12}$ cm^{-3}, $R = 4 \times 10^{14}$ cm and those shown for $n = 10^{10}$ cm^{-3}, $R = 4 \times 10^{15}$ cm.

The relatively flat incident spectrum means that Compton heating is dominated by the highest energies, $E_{\max}$. Balancing this heating (on the assumption of non-relativistic Compton scattering) with bremsstrahlung cooling gives an equilibrium temperature

$$T_{\rm eq} \simeq 3 \times 10^7 \mathrm{K} \left(\frac{L}{3 \times 10^{44}}\right)^2 \left(\frac{E_{\max}}{100\ \mathrm{keV}}\right)^2 \left(\frac{nR^2}{1.6 \times 10^{41}}\right)^{-2} \left(\frac{3(1-\alpha)}{2-\alpha}\right)^2,$$

where α is the energy spectral index. The computations yield final temperatures somewhat below $T_{\rm eq}$, owing to the reduction in the Compton heating rate due to the first-order Klein–Nishina corrections and the heating and cooling due to iron. The Klein–Nishina corrections also reduce the sensitivity of the gas temperature to $E_{\max}$.

We note that a higher density partial shell (or a collection of clouds) could mimic the observed spectrum. Then the absorption edges could be filled in by direct radiation seen through the gaps. Such holes would, however, reduce the computed ionization levels and require that the emission region lie at a smaller radius than that estimated for a complete shell.

3 Discussion

We have shown that a uniform shell of gas within 3×10^{16} cm of the nucleus of NGC 5548 may be photoionized to a state where it produces detectable iron line emission. The gas responsible has an electron scattering depth of about 2 and is Compton heated to a temperature of $\sim 2 \times 10^7$ K. Radio emission from within this region will be undetectable owing to free–free absorption. Weymann (1970) has discussed the dispersive effect of electron scattering in a cooler gas on the optical line profiles of NGC 5548. In our case the lines undergo a net blueshift equivalent to a Doppler shift of ~ 4000 km s^{-1} per scattering. A lack of any clear evidence of this effect indicates that most of the optical broad-line emission region lies beyond the X-ray line emitting region.

An electron scattering depth of 2 may arise in either an inflow or outflow of gas. A freely-falling accretion flow onto a black hole of mass M, where the kinetic energy is all released as 10^{44} erg s^{-1} of radiation at 3 Schwarzschild radii, yields $\tau \simeq 3 \times 10^6 (M/M_\odot)^{-1}$. A mass of $\sim 10^6 M_\odot$ gives the observed value of τ, and is then radiating close to its Eddington limit. This can, however, be ruled out since the product $nR^2 \ll 10^{41}$ cm^{-1} in the region where $\tau > 1$. A reduction in the radiative efficiency of the accretion flow, and/or of the inflow velocity (perhaps as a result of radiation pressure), can lead to an optically thicker flow at all radii.

The presence of an optically thick shell of gas surrounding a galactic nucleus modifies the hard X-ray continuum by Compton scattering. Bremsstrahlung from this gas can lead to an apparent low-energy excess, such as observed by Mushotzky *et al.* (1980) in ESO 141–G55.

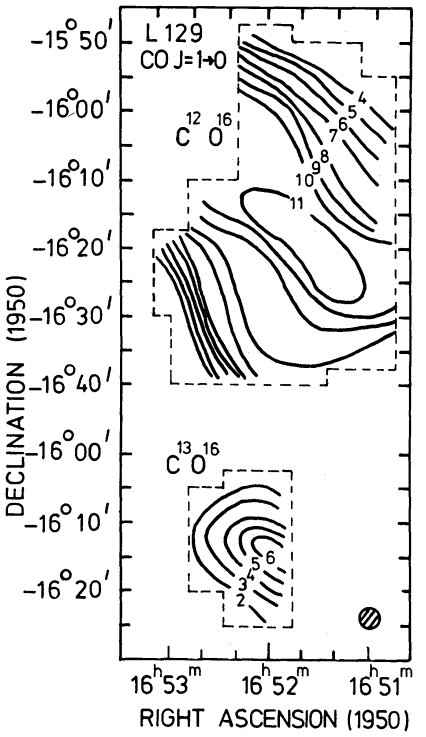

Figure 11. Peak $T_A^*(CO)$, $T_A^*(^{13}CO)$ for region of L129.

isothermal, a property to be expected where there is no appreciable internal heating source (see Appendix). The steep decline in $T(CO)$ at plateau limits presumably defines the physical limits of the cloud. ^{13}CO linewidth at the central core is comparable with expected free-fall velocity, and the dynamical time-scale for collapse is $\sim 5 \times 10^5$ yr.

The central core appears therefore to represent a density enhancement similar to that postulated for TMC-1 in the pre-shock regime.

9 Conclusions

Data and analysis have been presented for the dark clouds L1333, Heiles 2 (TMC-1), L1778 and L129. The observational characteristics of Heiles 2 suggest that a Mach ~ 3 shock is probably responsible for compression of TMC-1, a small high density cloud with anomalous cyanopolyyne abundance.

The presence of two velocity components in L1333 may be again attributable to shock propagation, although the evidence in this case is less ambiguous. Whilst the overall stability of L1778 remains in doubt, L129 is characterized by a small central condensation roughly coincident with the region of high extinction, with at least some properties in common with those postulated for the pre-shock TMC-1. Where there is a population of such condensations, the passage of even relatively weak shocks may induce a wave of star formation, as post-shock compression leads to gravitational instability and collapse. It is interesting, however, to note that TMC-1 may have survived this stage, and is now a relatively prolific cyanopolyyne production zone. If grain surface-formation processes are predominant, then observed abundances near the NH_3 peak are consistent with a relatively short molecular formation period $\lesssim 10^6$ yr. The observed variation of $[NH_3]/[HC_5N]$ over TMC-1 suggests however that certain molecular destruction schemes not investigated by Allen & Robinson (1977)

A scattering shell will also smear the appearance of any variability in the central source. The observations shown in Fig. 1, together with *Ariel V* Sky Survey observations (Marshall, Warwick & Pounds 1981), indicate that significant changes occur in NGC 5548 on a time-scale of months. The detection of variability on a time-scale of less than one week would further limit the radius of the shell within the value of 3×10^{16} cm derived from photo-ionization. We conclude that the iron line in this Seyfert galaxy is the innermost feature yet discerned in a galactic nucleus.

Acknowledgments

We thank L. Culhane and J. Bell-Burnell for a preprint of their observations and G. Ferland and M. Ward for discussions. ACF thanks the Radcliffe Trust for support. RRR acknowledges support by the National Science Foundation (grant PHY81-00605) and a NATO post-doctoral fellowship.

References

Bergeron, J., 1980. In *X-ray Astronomy*, p. 355, eds Giacconi, R. & Setti, G., D. Reidel, Dordrecht, Holland.

Blumenthal, G. & Mathews, W. G., 1979. *Astrophys. J.*, **233**, 479.

Hayes, M. J. C. Culhane, J. L., Blissett, R. J., Barr, P. & Bell Burnell, S. J., 1980. *Mon. Not. R. astr. Soc.*, **193**, 15P.

McCray, R., 1979. In *Active Galactic Nuclei*, p. 227, eds Hazard, C. & Mitton, S. Cambridge University Press.

Marsachi, L., Perola, G. C. & Treves, A., 1980. *Astrophys. J.*, **241**, 910.

Marshall, N., Warwick, R. S. & Pounds, K. A., 1981. *Mon. Not. R. astr. Soc.*, **194**, 984.

Mushotzky, R. F., Marshall, F. E., Boldt, E. A., Holt, S. S. & Serlemitsos, P. J., 1980. *Astrophys. J.*, **235**, 377.

Ross, R. R., 1978. *PhD thesis*, University of Colorado.

Ross, R. R., 1979. *Astrophys. J.*, **233**, 334.

Ulrich, M.-H., Boksenberg, A., Bromage, G., Carswell, R., Elvius, A., Gabriel, A., Gondalekar, P. M., Lind, J., Lindergren, L., Longair, M. S., Penston, M. V., Perryman, M. A. C., Pettini, M., Perola, G. C., Rees, M., Sciama, D., Snijders, M. A. J., Tanzi, E., Tarenghi, M. & Wilson, R., 1980. *Mon. Not. R. astr. Soc.*, **192**, 561.

Weymann, R. J., 1970. *Astrophys. J.*, **160**, 31.